

## Peak Power Management of Smart Grid Power Networks Using ESC for MPPT in PV Solar Systems

Gayatri Alaparthi

M.Tech Power Systems,

Department of Electrical & Electronics,

Newton's Institute of Engineering, Macherla. JNTUK.

B.Anji Babu, M.Tech

Assistant Professor,

Department of Electrical & Electronics,

Newton's Institute of Engineering, Macherla. JNTUK.

### Abstract:

Maximum Power Point Tracking(MPPT), controllers for solar inverters are flooding the market, these have encouraged a lot of customers move towards PV solar energy, because MPPT provides the boost required to maintain constant, voltage or current requirements. But the effectiveness of these systems are only optimal during the best weather conditions, and the fail to perform efficiently at varying weather conditions, they have weak transient response and output power loss. Extremum seeking control based MPPT systems, can efficiently solve these problems, to improve robustness during peak power production or peak power loads.

### Keywords:

PV - Photovoltaics, MPPT – Maximum Power Point Tracking, Extremum Seeking Control.

### I. Introduction:

The power surges in solar power plants, and the uncertainty in optimal climatic conditions, and various other factors have led to the research of Maximum Power Point Tracking, but this is a solved problem and universal. But there are issues related to MPPT in equatorial regions. This project was inspired by the conditions in India, the solar exposure level is not the same throughout the country, and the peak power production changes depending on it. If this problem of peak power management is solved, India would be benefited from the maintenance issues, the current power plants are facing. This will encourage more investors into solar power. The maximum efficiency of the modern solar cells is only around 30-40%, but this efficiency largely depends on the input radiation exposure, and the load characteristics of the cell.

So to improve the efficiency of the cells, the use of MPPT controllers is significant because it can handle the load requirements during the summer, but the methods for creating a MPPT controller are not universal, some are good at working only at peak conditions, while some require new solar panels, new batteries, or new super-capacitors. While this is not a disadvantage to many, it certainly is, in India the power plants, either owned by private companies or the government are reluctant to reinvest to buy new panels, every production cycle because, the efficiency gain doesn't justify the investment. So in this project, successfully attempts at providing a cost effective solution to solve this problem by using Extremum Seeking Control with MPPT. The simplified block diagram of the MPPT method is presented in the section II. Sinusoid extremum seeking control, is used for the paper and is presented in Section III. The detection block is an integral block, and is presented in the section IV. The dynamic stability of the system is explained and verified in Section V. The various models constructed in the scheme are described. Thus, the simulation of the sinusoid extremum seeking control is presented in Section VI. The conclusion of the paper is discussed in Section VII. The references are mentioned in Section VIII.

### II. Maximum Power Point Tracking:

With the change in the location of sun and the direction of the sun rays the power output of the solar power module changes. In Power vs. Voltage curve of the solar module there is only one maxima obtained of power which corresponds to the particular value of current and voltage.

Since the efficiency of the power module is less therefore it would be beneficial to operate it at the peak power point so that maximum power supply from the module can be achieved. Hence the maximization of power improves the utilization and reliability of the solar PV module.

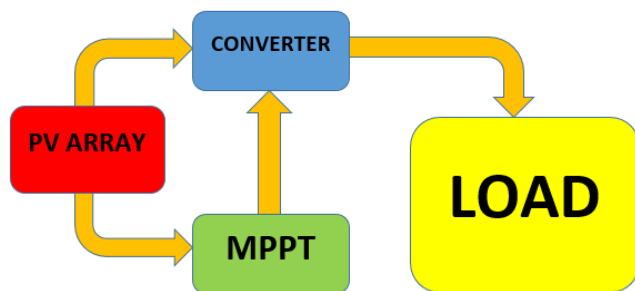


**Fig 1. Simplified Block Diagram of MPPT based converters.**

A maximum power point tracker (MPPT) technique is used to obtain the point of the maximum power from the solar PV module and transferring that power to the load. A dc to dc converter (step up/step down) is used for the purpose of transferring maximum power from the solar PV module utility grid. Maximum power point tracking is used to ensure that the panel output power is always achieved at the maximum power point. MPPT enables the enhancement of the solar based generation system. Using MPPT significantly increases the output power from the solar power plant. Losses in transformer, cabling, inverter and transmission systems, which can be easily measured in many cases. An IGBT based inverter is used to convert the dc supply received from PV array into the ac supply and thus which can be very easily fed into the utility grid or be used by the home appliances which are basically made to work on the ac supply. These inverters are used to connect the PV array to the grid through the transformers. These inverters use PWM technique and are IGBT based. The voltage versus current curves are shown in fig.5 for the solar module, the point of maximum power is achieved at the intersection of the current and voltage curve and at a particular value of irradiation received from the sun.

The efficiency of the inverter is measured on the basis of its ability to convert the ac into dc. Presently available inverters have efficiency of about 95 percent to 98.5percent and thus choice of correct inverter is very important aspect in the design process of power plant. The less efficient inverters can be used in the isolated systems or the grid tie. Inverters with efficiency less than 95percent are readily available in the market. Inverters when used at the low end of their maximum power are less efficient and therefore using the inverters at low end of maximum power should be avoided. Inverters are most efficient when used in the range of 30 to 90percent of power.

### III. SINUSOID EXTREMUM SEEKING CONTROL

The aim of the ESC is that the point known as operating point should be tending towards the ideal for undertaken system that has been described by not known nonlinear map with an only extreme point (i.e., a maximum or a minimum). Principle of the Sinusoid ESC, shown in Figure 2, can be condensed as mentioned: an input-output nonlinear map is shown, in continuation it is shown that a very small amplitude sinusoid signal is added to the x as an input signal, this yields y as the output signal which oscillate around its average value. If smaller input signal x is added than the maximum of the nonlinear map then both the sinusoid signal will be in phase and if larger input signal x is added than the maximum then both the sinusoid signal will be in counter phase, as it is shown in Figure 1. The Frequency of y as the output signal will be double if x as the input signal will reach maximum; it should also be noticed that the magnitude of the ripple of y as the output signal controlled by the curves gradient. It is also to be paid attention that, when y as the output signal is multiplied by the same frequency as well as same phase, the particular multiplier output g will be positive before the maximum had been reached and to the right of the maximum it will be negative.

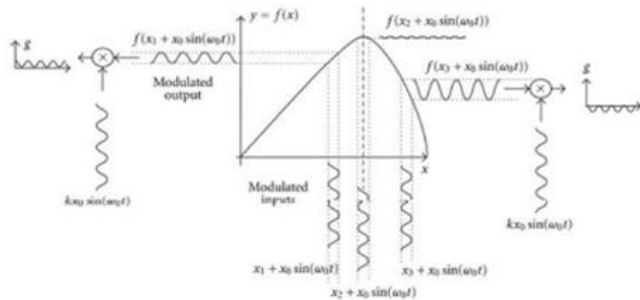


Fig 2. ESC Sinusoid Principle

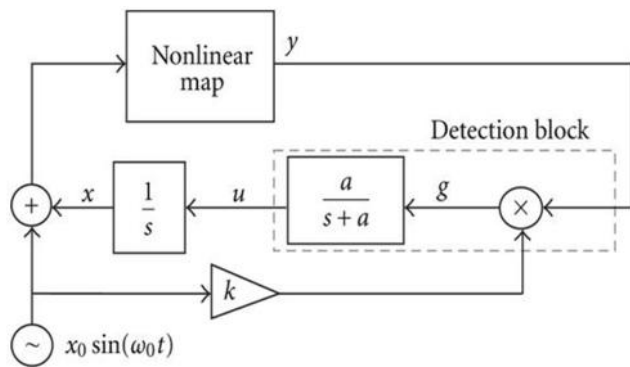


Fig 3. Block Diagram of ESC Principle

The following sections will describe the function of the detection block and examine the condition of stability, figure 2 shows the scheme.

**IV. DETECTION BLOCK:**

The output which comes out from the Detection block u being proportional to the slope of the map as described below. The integrator block output will have signal x and y as the output of the nonlinear mapping will be equated to

$$y = f(x + x_0 \sin(\omega_0 t)) \tag{1}$$

Sinusoid perturbation is considered small, assumed as the condition  $x_0 \ll x$ , then approximation of above expression by Taylor development will be as

$$y = f(x) + \frac{df(x)}{dx} x_0 \sin(\omega_0 t) \tag{2}$$

With the help of basic trigonometric identity,  $2\sin^2(\omega_0 t) = 1 - \cos(2\omega_0 t)$ , approximation of the output signal of the multiplier block will be as

$$\begin{aligned} g &= f(x) kx_0 \sin(\omega_0 t) + \frac{df(x)}{dx} kx_0^2 \sin^2(\omega_0 t) \\ &= \frac{1}{2} \frac{df(x)}{dx} kx_0^2 + f(x) kx_0 \sin(\omega_0 t) \\ &\quad - \frac{1}{2} \frac{df(x)}{dx} kx_0^2 \cos(2\omega_0 t) \end{aligned} \tag{3}$$

If it is considered that the first and second harmonics is attenuated by the low-pass filter completely, the expression of the output of the low-pass filter will be given as below

$$u = \frac{1}{2} \frac{df(x)}{dx} kx_0^2 * L^{-1} \left\{ \frac{a}{s+a} \right\} \tag{4}$$

Where \* is given as the convolution operator, and portion given in braces is the filter impulse response. Here, we have assumed small amplitude of the sinusoid perturbation and suitable attenuated harmonics, it should be declared that the output signal of the detection block i.e. u is proportional  $df(x)/dx$ , the slope of the curve.

**V. DYNAMIC STABILITY ANALYSIS:**

The only difference which is there in between the averaged signal and the real or the instantaneous signal is about the magnitude therefore with proper magnitude consideration analysis can be done. Averaged signals that is included in the sinusoid extremum-seeking circuit are

$$\begin{aligned} \bar{x} &= (1/T) \int_0^T (x + x_0 \sin(\omega_0 t)) dt \\ \bar{y} &= (1/T) \int_0^T y(t) dt \\ \bar{u} &= (1/T) \int_0^T u(t) dt \end{aligned}$$

$$\begin{aligned} T &= 2\pi/\omega_0 \\ \bar{y} &= \overline{f(x)}, \overline{f(x)} = f(\bar{x}) \end{aligned}$$

We obtain an average output of non-linear map, although according to expression (2), we can explain, here the dynamic relationship of averaged signals. This is shown with the help of Figure 3.

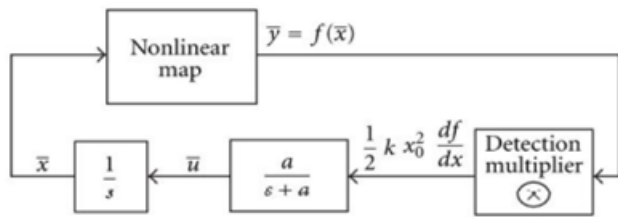


**Fig 4. Average – Signal Extremum seeking Control Block Diagram.**

Therefore, the constants term is denoted as,  $k_1 = kx_0^2/2$  and now the average dynamic behavior can be given as

$$\begin{aligned} \dot{\bar{x}} &= \bar{u}, \\ \dot{\bar{u}} &= -a\bar{u} + ak_1 \frac{df}{dx}, \end{aligned} \quad (5)$$

Where, the integrator differential equation is represented by row one whereas the filters differential equation is represented by row two. We have assumed that it has just one maximum and this show it behaviour as concave function; thus the evaluation of the second derivative or Hessian will give (less than zero) negative i.e.

$\frac{d^2 f}{dx^2} < 0$  It is seen that the when differentiated with respect to time the gradient gives

$$\frac{d}{dt} \left( \frac{df}{dx} \right) = \frac{d^2 f}{dx^2} \dot{\bar{x}} = \frac{d^2 f}{dx^2} \bar{u} \quad (6)$$

Renaming of the state variables is also an integral part and, the average dynamic system is expressed as

$$\begin{aligned} \dot{z}_1 &= h(z_1) z_2, \\ \dot{z}_2 &= -az_2 + ak_1 z_1, \end{aligned} \quad (7)$$

Where

$$\begin{aligned} z_1 &= df/dx \\ z_2 &= \bar{u}. \\ h(z_1) &= d^2 f/dx^2 < 0 \end{aligned}$$

Now we take care of the following candidate Lyapunov function to prove the stability condition of the nonlinear system,

$$V(z_1, z_2) = \frac{1}{2} z_2^2 + \int_0^{z_1} \left( -ak_1 \frac{1}{h(\alpha_1)} \alpha_1 \right) d\alpha_1$$

(8)

In order to verify the positive definiteness of  $V(z)$ , we see that the existence of a function which is continuous  $m(z_1)$  such that  $m(z_1)z_1 > 0$ , for all, implies

$$\int_0^{z_1} m(\alpha_1) d\alpha_1 > 0$$

It can be corroborated given that it is true for positive and negative  $Z_1$ , that is,

$$\begin{aligned} z_1 > 0 &\implies m(\alpha_1) > 0, \\ \alpha_1 \in (0, z_1) &\implies \int_0^{z_1} m(\alpha_1) d\alpha_1 > 0, \\ z_1 < 0 &\implies m(\alpha_1) < 0, \\ \alpha_1 \in (z_1, 0) &\implies \int_0^{z_1} m(\alpha_1) d\alpha_1 = - \int_{z_1}^0 m(\alpha_1) d\alpha_1 > 0 \end{aligned} \quad (9)$$

Now the function  $m(z_1)$  as  $m(z_1) = -ak_1(1/h(z_1))z_1$  it is observed that since  $a > 0$ ,  $k_1 > 0$  and,  $h(z_1) < 0$  then  $m(z_1)z_1 > 0$  for all  $z_1$  except  $z_1 = 0$ . Therefore,

$\int_0^{z_1} (-ak_1(1/h(\alpha_1))\alpha_1) d\alpha_1 > 0$  and thus  $V(z_1, z_2)$  is, positive definite.

Continuing further the derivating  $V(z_1, z_2)$  with respect to time gives

$$\dot{V}(z_1, z_2) = z_2 \dot{z}_2 + \left( -ak_1 \frac{1}{h(z_1)} z_1 \right) \dot{z}_1. \quad (10)$$

By the substitution of the state variables derivatives as per expression (7) in the time derivative of the Lyapunov function, (10) can be arranged as

$$\dot{V}(z_1, z_2) = -az_2^2 \quad (11)$$

As shown that  $V(Z_1, Z_2)$  is positive definite and  $\dot{V}(Z_1, Z_2)$  is semi negative definite, the condition thus proves the stability of the system. In regard to above it is easy to evaluate the asymptotic stability of the system, with the help of LaSalle invariance principle since origin is the only invariant of system for which  $\dot{V} = 0$ .

As assumed that the nonlinear map has just one maximum i.e.  $d^2 f/dx^2 < 0$ . The nonlinear map corresponds to the power-voltage curve of a PV panel has just one maxima. The section given below describes the adaptation technique to analyse the algorithm of MPPT circuit for a PV system. Moreover, thus a stable system is ensured and thus it is reliable for the operational range of the PV system. Analysis that can only considered is the stability in front of signal disturbances that is small can be found in.

### VI. SIMULATION OF SINUSOID EXTREMUM-SEEKING CONTROL:

As Shown in Figure 5, the time responses of a Sin ESC system under uniform irradiance of 1 kW/m<sup>2</sup> at 25 °C and variance drop to 600 W/m<sup>2</sup> at some time duration. It is found that large oscillation of the original ESC system is enhanced by introducing sinusoid perturbation and the MPP is precisely tracked as intended. The small residual oscillation during the transient state is added to the ESC system itself as well as the sinusoid perturbation. Therefore, it will result in large oscillation due to an increase in the amount of sinusoid perturbation, which need the parameter tuning to be reduced and hence the steady-state oscillations will be reduced. Figure 6 shows the simulations model in the case of reduction in irradiance from 1 kW/m<sup>2</sup> to 600 W/m<sup>2</sup> at some time duration. No matter how suddenly irradiance changes, the MPP can still be precise while tracking as shown in the previous case, this causes oscillation within acceptable range in the time duration = 10 s. It is proved that the Sin ESC approach do intend to improve the high oscillations as experienced in a conventional ESC approach. Figure 7 and figure 8 show the plots of the voltage and current waveforms respectively of the simulations done in figure 5 and 6.

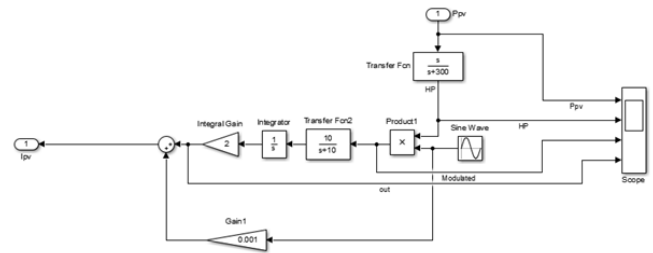


Fig 5. ESC – MPPT model Block in simulink

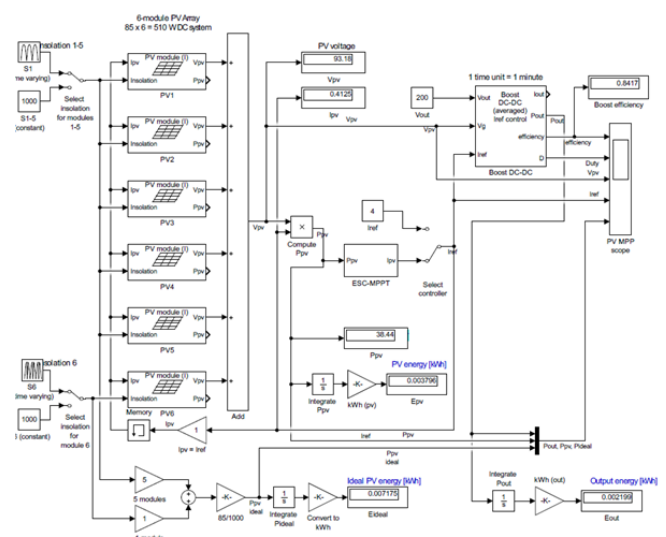


Fig 6. Simulink Simulation model of PV arrays, with Constant and time varying climatic conditions, and the output efficiency with ESC MPPT.

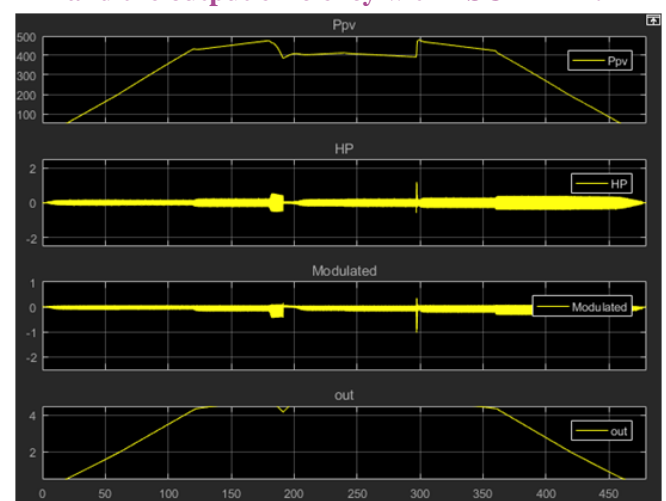


Fig 7. Simulated output of ESC - MPPT controller.

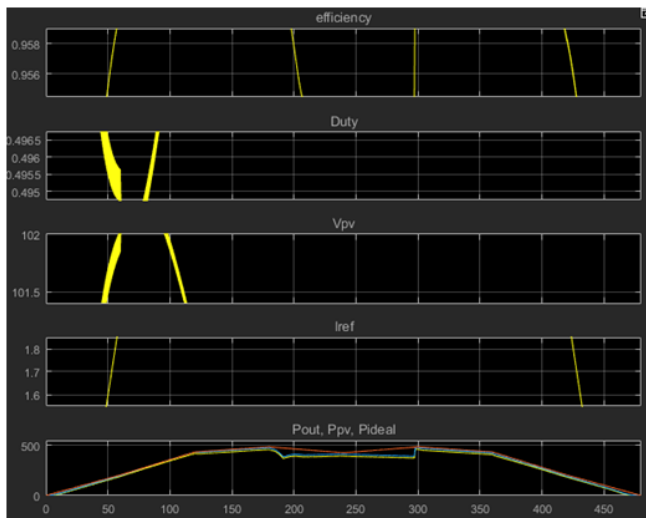


Fig 8. Power output, Duty, Voltage, current, and efficiency of the simulated system.

REFERENCES:

[1] E. Koutroulis, K. Kalaitzakis, and N. C. Voulgaris, “Development of a microcontroller-based, photovoltaic maximum power point tracking control system,” *IEEE Trans. Power Electron.*, vol. 16, no. 1, pp. 46–54, Jan. 2001.

[2] T. Eram and P. L. Chapman, “Comparison of photovoltaic array maximum power point tracking techniques,” *IEEE Trans. Energy Convers.*, vol. 22, no. 2, pp. 439–449, Jun. 2007.

[3] N. Femia, G. Petrone, G. Spagnuolo, and M. Vitelli, “Optimization of perturb and observe maximum power point tracking method,” *IEEE Trans. Power Electron.*, vol. 20, no. 4, pp. 963–973, Jul. 2005.

[4] N. Femia, D. Granozio, G. Petrone, G. Spagnuolo, and M. Vitelli, “Predictive & adaptive MPPT perturb and observe method,” *IEEE Trans. Aerosp. Electron. Syst.*, vol. 43, no. 3, pp. 934–950, Jul. 2007.

[5] A. Pandey, N. Dasgupta, and A. K. Mukerjee, “High-performance algorithms for drift avoidance and fast tracking in solar MPPT system,” *IEEE Trans. Energy Convers.*, vol. 23, no. 2, pp. 681–689, Jun. 2008.

[6] D. Sera, R. Teodorescu, J. Hantschel, and M. Knoll, “Optimized maximum power point tracker for fast-changing environmental conditions,” *IEEE Trans. Ind. Electron.*, vol. 55, no. 7, pp. 2629–2637, Jul. 2008.

[7] N. Femia, G. Petrone, G. Spagnuolo, and M. Vitelli, “A technique for improving P&O MPPT performances of double-stage grid-connected photovoltaic systems,” *IEEE Trans. Ind. Electron.*, vol. 56, no. 11, pp. 4473–4482, Nov. 2009.

[8] S. L. Brunton, C. W. Rowley, S. R. Kulkarni, and C. Clarkson, “Maximum power point tracking for photovoltaic optimization using ripple-based extremum seeking control,” *IEEE Trans. Power Electron.*, vol. 25, no. 10, pp. 2531–2540, Oct. 2010.

[9] F. Zhang, K. Thanapalan, A. Procter, S. Carr, and J. Maddy, “Adaptive hybrid maximum power point tracking method for a photovoltaic system,” *IEEE Trans. Energy Convers.*, vol. 28, no. 2, pp. 353–360, Jun. 2013.

[10] K. L. Lian, J. H. Jhang, and I. S. Tian, “A maximum power point tracking method based on perturb-and-observe combined with particle swarm optimization,” *IEEE J. Photovoltaics*, vol. 4, no. 2, pp. 626–633, Mar. 2014.

[11] Y. Levron and D. Shmilovitz, “Maximum power point tracking employing sliding mode control,” *IEEE Trans. Circuits Syst.*, vol. 60, no. 3, pp. 724–732, Mar. 2013.

[12] M. A. Elgendy, B. Zahawi, and D. J. Atkinson, “Assessment of the incremental conductance maximum power point tracking algorithm,” *IEEE Trans. Sustain. Energy*, vol. 4, no. 1, pp. 108–117, Jan. 2013.

[13] L. Cristaldi, M. Faifer, M. Rossi, and S. Toscani, “An improved model-based maximum power point

tracker for photovoltaic panels,” *IEEE Trans. Instrum. Meas.*, vol. 63, no. 1, pp. 63–71, Jan. 2014.

[14] J.-S. R. Jang, “ANFIS: Adaptive-network-based fuzzy inference system,” *IEEE Trans. Syst. Man Cybern.*, vol. 23, no. 3, pp. 665–685, May/Jun. 1993.

[15] M. Veerachary, T. Senjyu, and K. Uezato, “Feedforward maximum powerpoint tracking of PV systems using fuzzy controller,” *IEEE Trans. Aerosp. Electron. Syst.*, vol. 38, no. 3, pp. 969–981, Jul. 2002.

[16] M. A. A. M. Zainuri<sup>1</sup>, M. A. M. Radzi<sup>1</sup>, A. C. Soh<sup>1</sup>, and N. Abd Rahim, “Development of adaptive perturb and observe-fuzzy control maximum power point tracking for photovoltaic boost dc–dc converter,” *IET Renew. Power Gener.*, vol. 8, no. 2, pp. 183–194, Mar. 2014.

[17] A. Chikh and A. Chandra, “Adaptive neuro-fuzzy based solar cell model,” *IET Renew. Power Gener.*, vol. 8, no. 6, pp. 679–686, Aug. 2014.

[18] J.-S. R. Jang, C.-T. Sun, and E. Mizutani, *Neuro-Fuzzy and Soft Computing*. Englewood Cliffs, NJ, USA: Prentice-Hall, 1997. [19] H. P. Desai and H. K. Patel, “Maximum power point algorithm in PV generation: An overview,” in *Proc. 7th Int. Conf. Power Electron. Drive Syst. (PEDS’07)*, 2007, pp. 624–630.

[20] C. W. Tan, T. C. Green, and C. A. Hernandez-Aramburo, “An improved maximum power point tracking algorithm with current-mode control for photovoltaic applications,” in *Proc. IEEE Int. Conf. Power Electron. Drives Syst.*, 2005, pp. 489–494.

[21] Y. Yusof, S. H. Sayuti, M. Abdul Latif, and M. Z. Che Wanik, “Modeling and simulation of maximum power point tracker for photovoltaic system,” in *Proc. Nat. Power Energy Conf. (PECon)*, Kuala Lumpur, Malaysia, 2004, pp. 88–93.

[22] J. Ho Lee, H. Bae, and B. H. Cho, “Advanced incremental conductance MPPT algorithm with a variable step size,” in *Proc. 12th Int. Power Electron. Motion Control Conf. (EPE-PEMC’06)*, Portoroz, Slovenia, Aug. 30/Sep. 1, 2006, pp. 603–607.

[23] B. Liu, S. Duan, F. Liu, and P. Xu, “Analysis and improvement of maximum power point tracking algorithm based on incremental conductance method for photovoltaic array,” in *Proc. 7th Int. Conf. Power Electron. Drive Syst. (PEDS’07)*, Bangkok, Thailand, Nov. 27–30, 2007, pp. 637–641.

[24] Z. Yan, L. Fei, Y. Jinjun, and D. Shanxu, “Study on realizing MPPT by improved incremental conductance method with variable step-size,” in *Proc. IEEE 3th Ind. Electron. Appl. Conf.*, 2008, pp. 547–550.

[25] A. Chikh and A. Chandra, “An optimum method for maximum powerpoint tracking in photovoltaic systems,” in *Proc. IEEE Power Energy Soc. Gen. Meeting*, Detroit, MI, USA, 2011, pp. 1–6.

[26] K. Samangkool and S. Premrudeepreechacharn, “Maximum power point tracking using neural networks for grid-connected photovoltaic system,” in *Proc. Int. Conf. Future Power Syst.*, 2005, 4 pp.

[27] R. Ramaprabha<sup>1</sup>, B. L. Mathur, and M. Sharanya, “Maximum powerpoint tracking using GA-optimized artificial neural network for solar PV system,” in *Proc. 1st Int. Conf. Elect. Energy Syst. (ICEES)*, India, 2011, pp. 264–268.

[28] B. M. Wilamowski and X. Li, “Fuzzy system based maximum powerpoint tracking for PV system,” in *Proc. 28th IEEE Annu. Conf. Ind. Electron. Soc. (IECON’02)*, 2002, pp. 3280–3284.

[29] A. M. Subiyanto and M. A. Hannan, “Maximum power point tracking in grid connected PV system using a novel fuzzy logic controller,” in *Proc. Stud.*

Conf. Res. Develop. (SCORED'09), UPM Serdang, Malaysia, Nov.16–18, 2009, pp. 349–352.

[30] L. Chun-hua, J. Xu, and Z. Xin-jian, “Study on control strategy for photovoltaic energy systems based on recurrent fuzzy neural networks,” in Proc. 5th Int. Conf. Nat. Comput., 2009, pp. 282–286.

[31] X. Yang and C. Zeng, “Generalized dynamic fuzzy neural network-based tracking control of PV,” in Proc. Asia-Pac. Power Energy Eng. Conf. (APPEEC), 2010, pp. 1–4.

[32] N. Khaehintung, P. Sirisuk, and W. Kurutach, “A novel ANFIS controller for maximum power point tracking in photovoltaic systems,” in Proc. 5<sup>th</sup> Int. Conf. Power Electron. Drive Syst. (PEDS'03), 2003, pp. 833–836.

[33] C. A. Otieno, G. N. Nyakoe, and C. W. Wekesa, “A neural fuzzy based maximum power point tracker for a photovoltaic system,” in Proc. IEEE Conf. (AFRICON'09), Nairobi, Kenya, Sep. 23–25, 2009, pp. 1–6.

[34] A. Chikh and A. Chandra, “Optimization and control of a photovoltaic powered water pumping system,” in Proc. IEEE Elect. Power Energy Conf. (EPEC), Montreal, Canada, 2009, pp. 1–6.

[35] A. Chikh and A. Chandra, “Voltage and frequency controller for a standalone PV system with battery storage element,” in Proc. 38th Annu. Conf. IEEE Ind. Electron. Soc. (IECON'12), Montreal, Canada, Oct. 25–28, 2012, pp. 1172–1177.

[36] A. Chikh and A. Chandra, “Sizing and power management for a standalone PV system in cold climate,” in Proc. IEEE PES Transm. Distrib. Conf. Expo. (T&D), May 7–8, 2012, pp. 1–6.

[37] H. Liu, G. Liu, and Y. Shen, “A novel harmonics detection method based on wavelet algorithm for active

power filter,” in Proc. 6th World Congr. Intell. Control Autom., China, Jun. 21–23, 2006, pp. 7617–7621.

[38] S. G. Mihov, R. M. Ivanov, and A. N. Popov, “Denoising speech signals by wavelet transform,” Annu. J. Electron., pp. 1–6, 2009, ISSN 1313-1842.

[39] J. Ning and W. Gao, “Continuous wavelet-based active filter design for harmonic mitigation in hybrid electric vehicles,” in Proc. IEEE Conf. Veh. Power Propul., Michigan, Sep. 7–11, 2009, pp. 859–865.

[40] H. T. Yalazan, T. Sürgevil, and E. Akpınar, “Wavelet transform application in active power filter used for slip energy recovery drives,” in Proc. Int. Aegean Conf. Elect. Mach. Power Electron., Turkey, Sep. 10–12, 2007, pp. 398–403.

[41] A. H. Ghaemi, H. Askarian Abyaneh, K. Mazlumi, and S. H. H. Sadeghi, “Voltage notch indices determination using wavelet transform,” in Proc. IEEE Powertech, Switzerland, Jul. 1–5, 2007, pp. 80–85.

[42] K. H. Kashyap and U. J. Shenoy, “Classification of power system faults using wavelet transforms and probabilistic neural networks,” in Proc. Proc. Int. Symp. Circuits Syst. (ISCAS'03), Bangkok, May 25–28, 2003, pp. 423–426.

[43] <http://www.mrsolar.com/content/pdf/Solartech/>